SUPPORTING INFORMATION

Scanning electrochemical cell microscopy (SECCM) in a glovebox: Structure-activity correlations in the early stages of solid-electrolyte interphase (SEI) formation on graphite

Daniel Martín-Yerga[1,3*], Minkyung Kang[1,2], Patrick R. Unwin[1,3*]

[1]*Department of Chemistry, University of Warwick, Coventry CV47AL, United Kingdom*

[2]*Institute for Frontier Materials, Deakin University, Burwood VIC 3125, Australia*

[3]*The Faraday Institution, Quad One, Harwell Campus, Didcot OX11 0RA, United Kingdom*

*Corresponding authors: daniel.martin-yerga@warwick.ac.uk (D.M-Y); p.r.unwin@warwick.ac.uk (P.R.U.)

SECTION S1. ADDITIONAL FIGURES

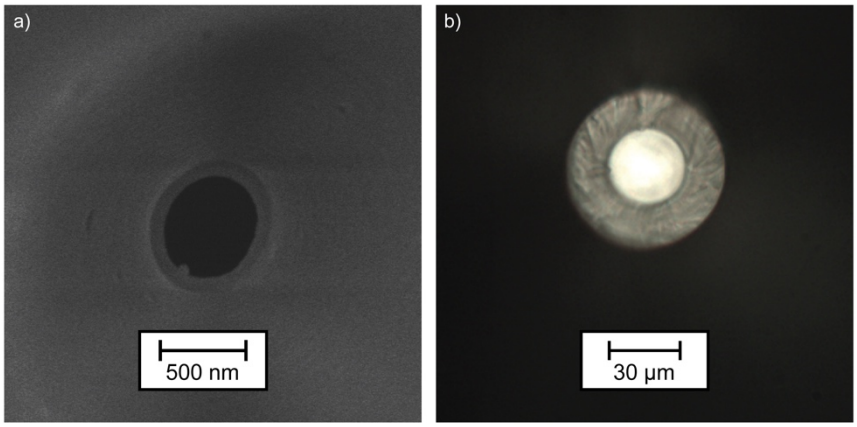

Figure S1. (a) SEM image of a representative nanopipette probe with a diameter of ca. 500 nm. (b) Optical microscopic image of a representative micropipette probe with diameter of ca. 30 µm.

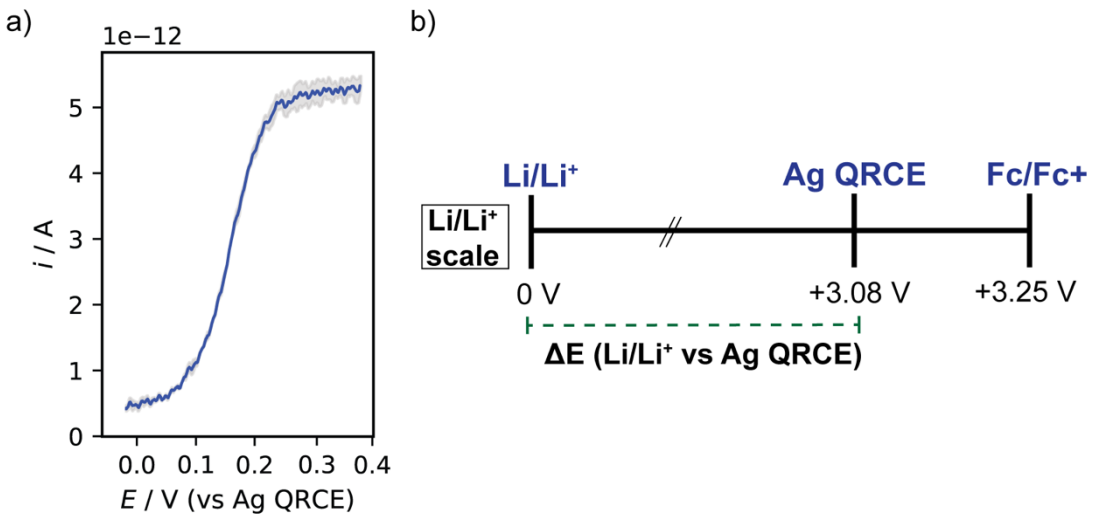

Figure S2. (a) Average SECCM CV (n=9) for the oxidation of 3 mM Fc in 1 M $LiPF_6$ in EC/EMC. $E_{1/2}$ for the Fc^0/Fc^+ process was +0.17 V vs Ag QRCE. Scan rate was 1 V s^{-1}. (b) Conversion scale used between Li/Li^+ and the Ag QRCE, where a potential for Fc^0/Fc^+ of +3.25 V vs Li/Li^+ was considered as reported previously in the same electrolyte and solvent.[1]

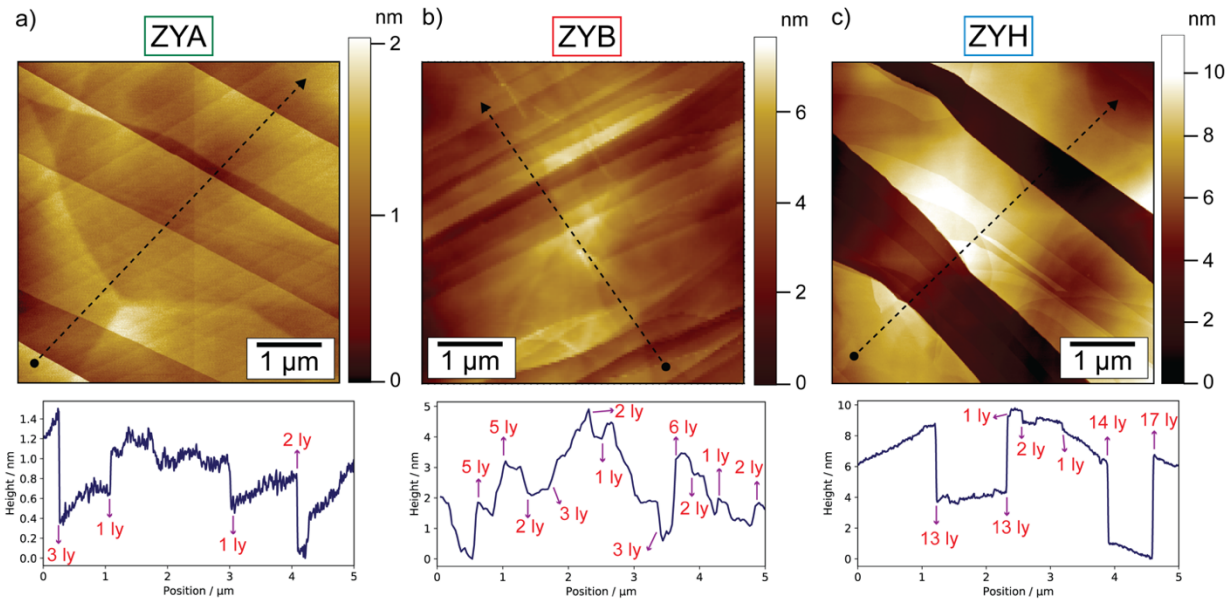

Figure S3. Additional AFM topography images of freshly cleaved HOPG with corresponding height profiles for (a) ZYA, (b) ZYB, and (c) ZYH grades. Arrows indicate the location and direction where the height profiles were extracted. "ly" indicates graphite layer.

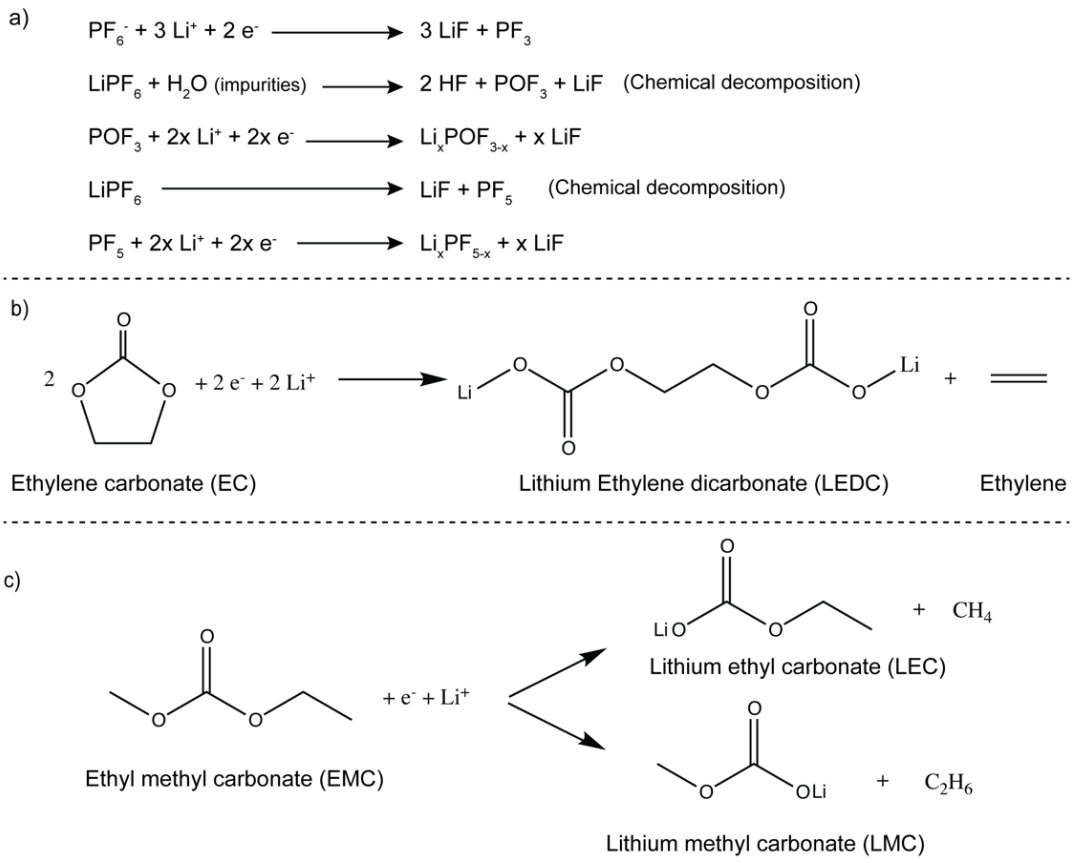

Figure S4. Initial reactions expected to take place on graphite surfaces during electrochemical reduction of electrolyte salt ($LiPF_6$) and solvents (EC, EMC) according to previous literature.[2–6] Some products from these initial reactions can also undergo subsequent chemical and electrochemical reactions until generating stable products.

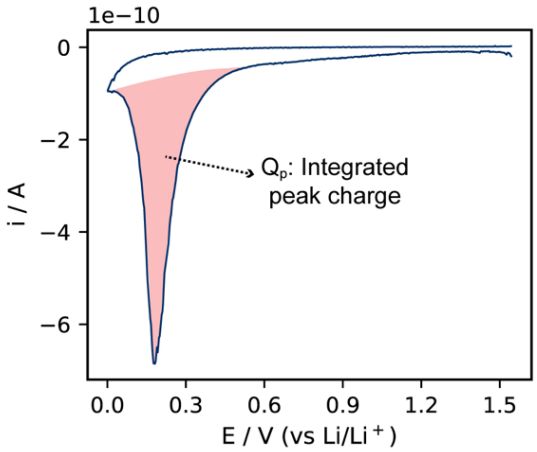

Figure S5. Cyclic voltammetry plot showing how the peak charge (Q_p) was integrated to carry out the data analysis for all the results described in this work.

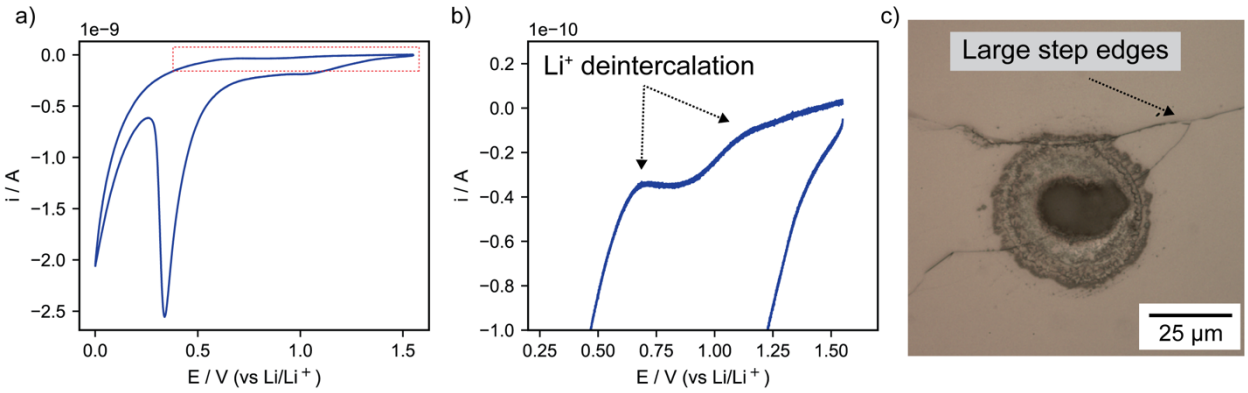

Figure S6. (a) SECCM cyclic voltammetry measurement in 1 M $LiPF_6$ in EC/EMC recorded with a pipette of ~30 µm diameter. Scan rate was 50 mV s^{-1}. (b) Zoomed-in area of the CV highlighting the Li^+ deintercalation processes. (c) Optical image of the droplet footprint left by the SECCM experiment showing the large graphite defects (step edges) covered by the pipette footprint (electrolyte droplet) during the experiment.

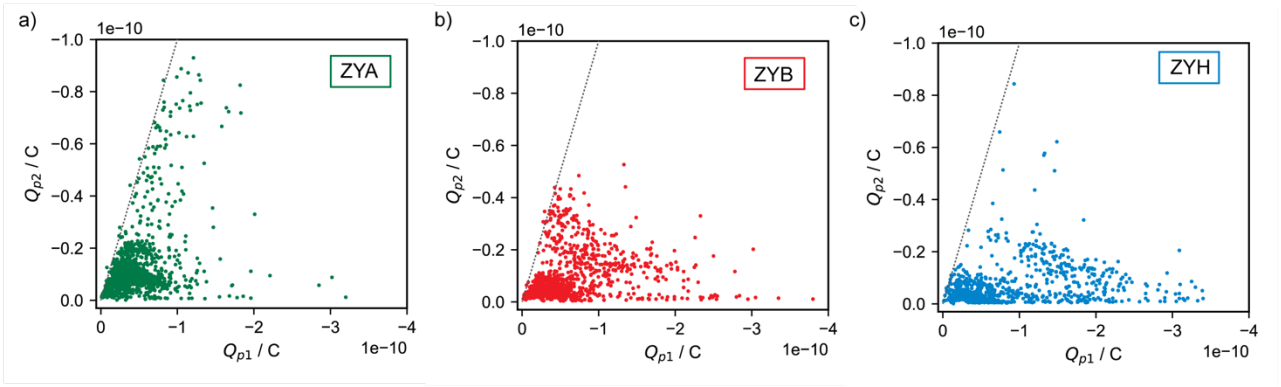

Figure S7. Relationship between Q_{p1} and Q_{p2} for ZYA, ZYB and ZYH HOPG electrodes at 1 V s^{-1}. Dashed line represents values where Q_{p1} is equal to Q_{p2} (Q_{p2}/Q_{p1} = 1; no SEI passivation).

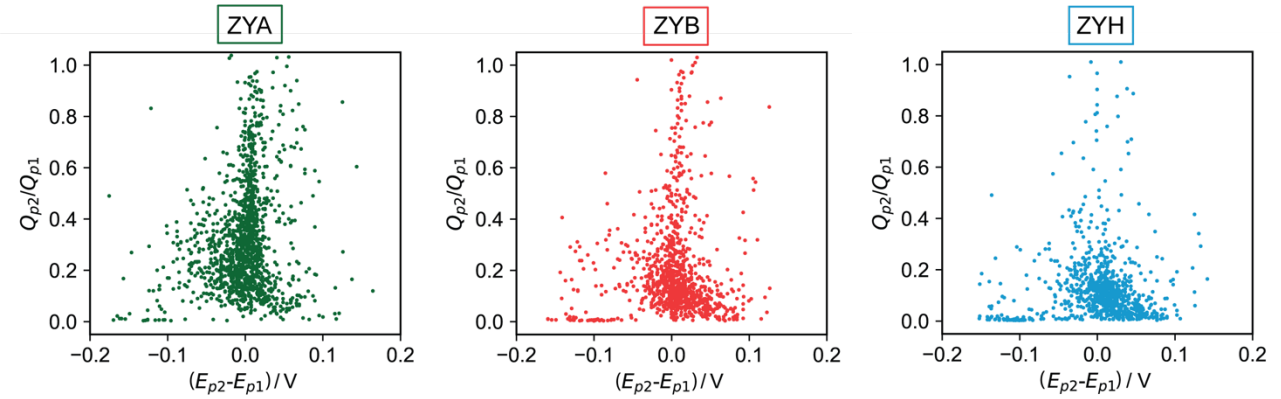

Figure S8. Relationship between Q_{p2}/Q_{p1} and (E_{p2}-E_{p1}) for ZYA, ZYB, and ZYH HOPG electrodes at 1 V s^{-1}.

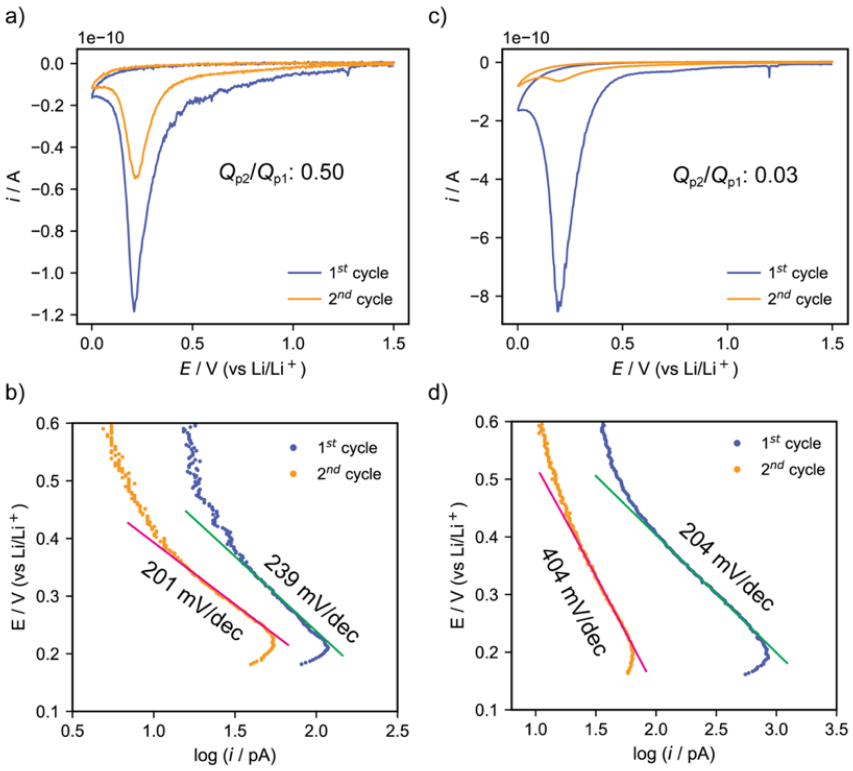

Figure S9. CVs (a, c) and corresponding Tafel plots (b, d) (recorded at two different locations of a ZYB HOPG in 1 M $LiPF_6$ in EC/EMC at a scan rate of 1 V s^{-1} (1st cycle: blue line, 2nd cycle: orange line). CVs represent locations where different values of Q_{p2}/Q_{p1} (i.e., SEI passivation efficiency) were obtained: (a) 0.50, (c) 0.03.

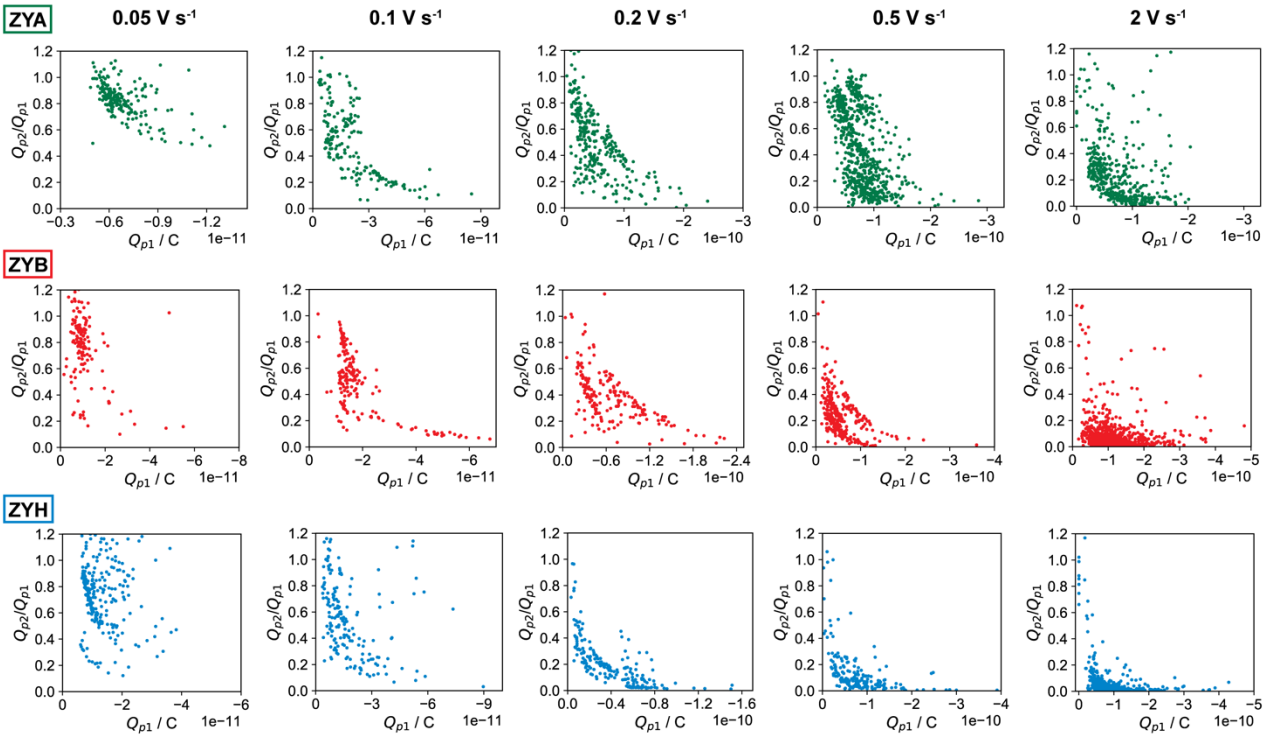

Figure S10. Plots of Q_{p2}/Q_{p1} vs Q_{p1} for ZYA, ZYB, and ZYH HOPG at various scan rates: 0.05, 0.1, 0.2, 0.5, 1 and 2 V s^{-1}.

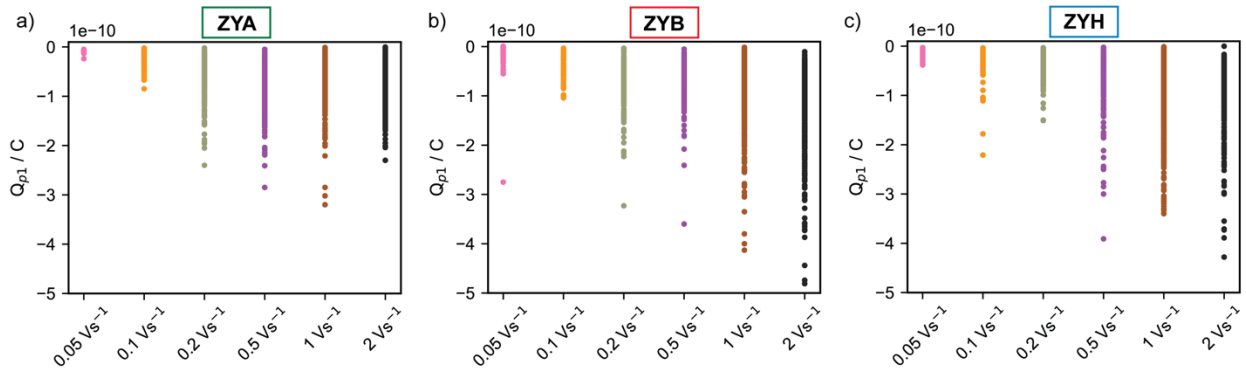

Figure S11. Plots of all Q_{p1} values obtained from the SECCM experiments as a function of scan rate for (a) ZYA, (b) ZYB, and (c) ZYH HOPG electrodes.

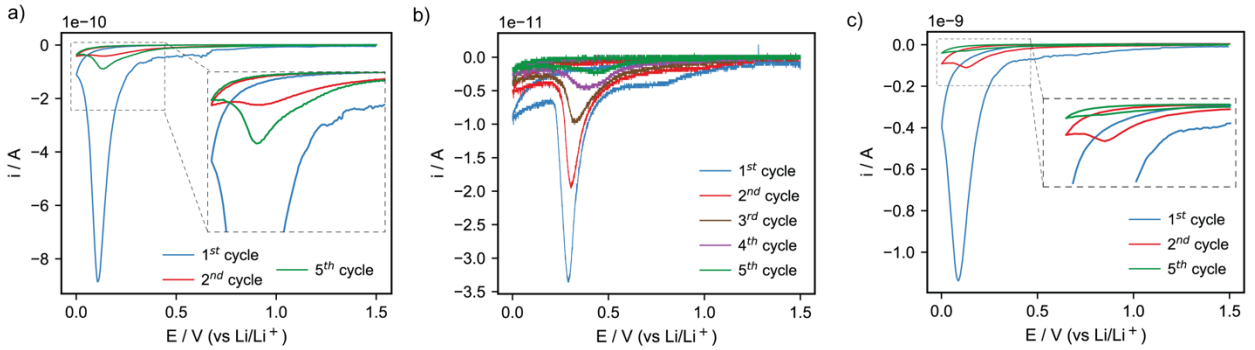

Figure S12. Multi-cycling CVs representing typical cases where the SEI was (a) less passivating in the 5th cycle than the 2nd cycle (Q_{p5}/Q_{p2}: 2.9, Q_{p2}/Q_{p1}: 0.03) at intermediate scan rates (1 V s^{-1}); (b) increasingly passivating (Q_{p5}/Q_{p2}: 0.13, Q_{p2}/Q_{p1}: 0.63) upon cycling at slow scan rates (0.05 V s^{-1}), and (c) more passivating in the 5th cycle than the 2nd cycle (Q_{p5}/Q_{p2}: 0.19, Q_{p2}/Q_{p1}: 0.10) at fast scan rates (2 V s^{-1}). Data recorded on ZYB HOPG electrodes.

SECTION S2. SECCM PROBE PULLING PARAMETERS

Single-channel probes of ca. 500 nm diameter

Pipette puller: P2000 (Sutter Instruments)

Capillaries: GC120F-10 (Harvard Apparatus) with 0.69 and 1.2 mm inner and outer diameters, respectively.

Program:

Line 1: HEAT 350, FIL 3, VEL 40, DEL 220, PUL 0

Line 2: HEAT 350, FIL 3, VEL 40, DEL 180, PUL 100

Single-channel probes of ca. 30 µm diameter:

Pipette puller: PC-10 (Narishige Group)

Capillaries: GC100F-75 (Harvard Apparatus) with 0.58 and 1.0 mm inner and outer diameters, respectively.

Program:

1st step: HEATER 70, WEIGHT 3, SLIDER 8

2nd step: HEATER 55, WEIGHT 3, SLIDER 4

SECTION S3. REFERENCES

(1) Laoire, C. O.; Plichta, E.; Hendrickson, M.; Mukerjee, S.; Abraham, K. M. Electrochemical Studies of Ferrocene in a Lithium Ion Conducting Organic Carbonate Electrolyte. *Electrochimica Acta* **2009**, *54* (26), 6560–6564. https://doi.org/10.1016/j.electacta.2009.06.041.

(2) Agubra, V. A.; Fergus, J. W. The Formation and Stability of the Solid Electrolyte Interface on the Graphite Anode. *J. Power Sources* **2014**, *268*, 153–162. https://doi.org/10.1016/j.jpowsour.2014.06.024.

(3) Heiskanen, S. K.; Kim, J.; Lucht, B. L. Generation and Evolution of the Solid Electrolyte Interphase of Lithium-Ion Batteries. *Joule* **2019**, *3* (10), 2322–2333. https://doi.org/10.1016/j.joule.2019.08.018.

(4) Nie, M.; Chalasani, D.; Abraham, D. P.; Chen, Y.; Bose, A.; Lucht, B. L. Lithium Ion Battery Graphite Solid Electrolyte Interphase Revealed by Microscopy and Spectroscopy. *J. Phys. Chem. C* **2013**, *117* (3), 1257–1267. https://doi.org/10.1021/jp3118055.

(5) Seo, D. M.; Chalasani, D.; Parimalam, B. S.; Kadam, R.; Nie, M.; Lucht, B. L. Reduction Reactions of Carbonate Solvents for Lithium Ion Batteries. *ECS Electrochem. Lett.* **2014**, 3.

(6) Wang, Y.; Nakamura, S.; Ue, M.; Balbuena, P. B. Theoretical Studies To Understand Surface Chemistry on Carbon Anodes for Lithium-Ion Batteries: Reduction Mechanisms of Ethylene Carbonate. *J. Am. Chem. Soc.* **2001**, *123* (47), 11708–11718. https://doi.org/10.1021/ja0164529.